ACS FOOD SCIENCE & TECHNOLOGY

Open Access

pubs.acs.org/acsfoodscitech

Article

Matrix-Dependent Remodeling of an RG-I-Rich Pectin Fraction during INFOGEST Digestion of Golden Delicious Apples: Intact Pulp vs Processed Homogenate

Clara Comuzzi,* Marilisa Alongi, Umberto Lanza, Asja Brovedani, Erica Moret, Lara Manzocco, and Maria Cristina Nicoli

Cite This: https://doi.org/10.1021/acsfoodscitech.6c00023

Read Online

ACCESS | Metrics & More | Article Recommendations | Supporting Information

ABSTRACT: The gastrointestinal structural fate of pectin is a key determinant of its nutritional relevance; however, most available studies rely on isolated polymers and do not account for the influence of the native food matrix. Here, we tested whether the apple tissue state governs post-digestive remodeling of an RG-I-rich pectic fraction during in vitro gastrointestinal digestion (INFOGEST), comparing intact Golden Delicious apple pulp with a processed homogenate. In undigested samples, the polymeric (>10 kDa) water-extracted RG-I-enriched pectic fraction (WERP) showed comparable RG-I fingerprints in both matrices. After digestion, a clear divergence emerged: pulp-derived WERP showed pronounced RG-I side-chain loss and an approximately order-of-magnitude decrease in apparent molecular weight, whereas homogenate-derived WERP largely retained its pre-digestive fingerprint. Digestion of isolated apple pectin did not reproduce these changes, consistent with a key role of tissue context and processing history.

KEYWORDS: *apple matrix, INFOGEST, indigestible residue, rhamnogalacturonan I (RG-I), arabinan, NMR spectroscopy*

1. INTRODUCTION

Apples are among the most widely consumed fruits worldwide and constitute a major dietary source of health-promoting compounds. Their beneficial properties are largely attributed to phenolic constituents and dietary fiber (DF), with pectin as the predominant fraction.[1−3] Pectin occurs in both soluble and insoluble forms within the cell wall; however, the soluble fraction is often considered a major contributor to its physiological effects, due to its higher fermentability and ability to modulate the gut microbiota and promote the formation of short-chain fatty acids (SCFAs).[4−6] These functional properties are tightly linked to pectin's structure.[7,8] In this respect, apple pectin is mainly composed of two domains: homogalacturonan (HG), a linear chain of α-1,4-linked galacturonic acid (GalA) residues with variable methyl-esterification, and rhamnogalacturonan I (RG-I), which consists of an alternating GalA−rhamnose backbone bearing neutral sugar side chains (arabinose- and galactose-rich) that may be branched.[9−11]

Notably, increasing evidence supports the RG-I domain as a key structural contributor to the reported pectin bioactivities in model systems, indicating that RG-I abundance and neutral-sugar side-chain architecture (e.g., degree of branching) are major determinants.[12,13] Consistently, RG-I-rich soluble fractions selectively stimulate specific microbial taxa and enhance SCFA production in fermentation models,[14−16] whereas features such as branching degree have been linked to immunomodulatory and anti-inflammatory effects.[17,18] However, current structure−function knowledge is largely based on isolated pectin. In contrast, the actual molecular substrates available for colonic fermentation after the upper gastrointestinal transit of the whole fruit matrix remain insufficiently defined. This is a critical point because microbial fermentation is expected to depend not simply on the native structure of pectin but on the molecular form in which pectic polymers reach the large intestine, whether as intact polymers or as depolymerized oligomeric fragments.[19]

Available digestion studies, including those in which the INFOGEST method is applied, generally report limited modification of pectins during the gastric and small-intestinal phases,[3,20−22] with the observed changes mainly involving the esterification pattern of GalA residues within the HG domain rather than major backbone or side-chain degradation.[23] However, such studies rely on purified substrates[22] and thus overlook the potential influence of the native fruit matrix. Although INFOGEST has also been applied to pectin-rich foods, these studies have mainly focused on matrix effects on digestion, bioaccessibility, or downstream fermentation, rather than on the post-digestive structural fate of tissue-embedded pectic polymers.[24−26] As a result, whether and how tissue-embedded pectins, particularly RG-I-rich populations, are structurally remodeled during digestion remain insufficiently explored. Recent studies on whole plant tissues and plant cell walls suggest that digestion can alter the extractability and accessibility of polysaccharide populations embedded within

Received: January 9, 2026
Revised: April 1, 2026
Accepted: April 1, 2026

the cell wall.[27,28] This may, in turn, modulate the accessibility of digestive fluids to pectic polymers and contribute to outcomes that differ from those observed in simplified substrate-only systems. Matrix-related effects may be further amplified by processing, which can markedly alter particle size, viscosity, pectin solubilization, and interactions with other cell wall components, thereby shaping the context in which pectin encounters gastrointestinal conditions.[29,30] High-pressure homogenization, in particular, has been shown to modify the side-chain architecture of pectins in citrus[31] and to influence pectin−cell wall interactions in apple-based products.[32] Nevertheless, how such processing-driven matrix differences translate into the molecular fate of pectin during digestion remains insufficiently defined, particularly for structurally complex domains such as RG-I. In light of these considerations, this study investigated whether processing-induced differences in the apple tissue state influence the structural fate of a polymeric (>10 kDa), water-extracted, (RG-I)-rich pectic fraction (WERP) during simulated digestion. Specifically, we compared intact pulp and a processed homogenate as two distinct tissue states expected to differ in cell−wall macrostructure and pectin−matrix interactions. Intact apple pulp and a processed apple homogenate were subjected to a standardized in vitro digestion protocol (INFOGEST), after which WERP was isolated and structurally characterized by gas chromatography (GC), nuclear magnetic resonance spectroscopy (NMR), and size-exclusion HPLC (SE-HPLC).

Digestion of isolated apple pectin under the same protocol was included to assess whether gastrointestinal conditions alone reproduced the transformations observed in tissue matrices. By linking the matrix state and processing history to post-digestive RG-I architecture, this study contributes to current knowledge beyond substrate-only digestion models, providing a domain-oriented view of how the food structure and digestion shape the molecular forms of pectin potentially available for colonic fermentation. The study also provides a basis for mechanistic hypotheses, including the possible contribution of tissue-associated enzymatic activities, which will require future verification.

2. MATERIALS AND METHODS

2.1. Sample Preparation

Golden Delicious apples were provided by Friul Fruct (Friulan Cooperative of fruit growers) at early commercial harvest maturity. Fruits were uniform in size (ca. 100−120 g), with green-yellow skin and free of visible defects. Upon receipt, fruits were stored at 4 °C and further processed within 1 week. For extraction purposes (see Section 2.2), several fruits were peeled, and the flesh was cut into thin slices and freeze-dried (Epsilon 2−4 LSCplus, Martin Christ GmbH, Osterode am Harz, Germany). Lyophilized samples were stored at −80 °C in the dark and processed within 2 weeks to ensure structural preservation of polysaccharides. Apple homogenate was prepared as described in previous work.[29] After washing and peeling, 5 mm thick slices were obtained from the pulp, sealed in polyamide−polyethylene pouches under vacuum (Combivac, Modena, Italy), blanched in boiling water for 3 min according to the literature[33,34] to inactivate apple endogenous enzymes, such as polyphenol oxidases and arabinofuranosidase, and cooled to 20 °C in an ice−water slurry. To produce the apple homogenate, apple pulp was first homogenized at a high speed at 20,000 rpm for 15 min and then subjected to three-pass high-pressure homogenization (HPH) at 20, 30, and 50 MPa (GEA Lab Homogenizer PandaPLUS 2000, GEA Group, Düsseldorf, Germany). The homogenate was then pasteurized at 100 °C for 6 min to obtain a 2-log reduction of *Alicyclobacillus acidoterrestris* (D90 = 7.4 min, z = 12 °C). These processing conditions resembled those typically used to obtain apple homogenate.[35,36] Homogenates were packed in PA/PE pouches, stored at −80 °C in the dark, and processed within 2 weeks to ensure structural preservation of polysaccharides. Homogenate samples intended for extraction were freeze-dried, stored at −80 °C in the dark, and processed within 2 weeks to ensure structural preservation of polysaccharides.

2.2. Pectin Extraction

The extraction protocol[37] consisted of a series of solubilization/precipitation steps, ensuring the structural preservation of the recovered pectin. The general procedure for extracting WERP is described below. Five grams of freeze-dried samples were added to 200 mL of an 80% ethanol (EtOH) solution (absolute ethanol VWR Chemicals, France) and refluxed for 1 h. The solid residue was filtered using Whatman filter paper (pore size 12−25 μm, Sigma-Aldrich, MO, USA), dried in an oven at 60 °C for 2 h, suspended in 100 mL of water, and brought to 80 °C for 20 min. After cooling at room temperature, the suspension was filtered and passed through a cation exchange resin pad (1 cm diameter × 5 cm height, Dowex 50W-X8, H^+, Sigma-Aldrich, MO, USA). After the filtrate was collected, the pad was rinsed with water (15 mL × 3), and the collected portions (ca. 130 mL) were concentrated (to ca. 25 mL) by evaporation under reduced pressure and then diluted with ethanol until an 80% solution was obtained. The solution was placed in the fridge for one night. The precipitated pectin was separated by filtration and dried in an oven at 60 °C for about 2 h. The sample was redissolved in 5 mL of water. The obtained solution was withdrawn and centrifuged through a filter with a 10,000 Da molecular weight cutoff (Sartorius, Goettingen, Germany). The filtrate (WERP filtrate) and the retentate (WERP fraction) were freeze-dried and finally stored in the freezer (−20 °C) until used for analysis. Hereafter, WERP refers to the operationally defined polymeric fraction retained above 10 kDa following the described extraction and purification workflow (Figure S1). Aliquots of 25 to 30 mg of WERP were obtained. The WERP extracted from apple pulp and apple homogenate were named respectively A_U (undigested) and H_U (undigested).

2.3. In Vitro Digestion

Apple pulp and homogenate were in vitro digested based on the standardized INFOGEST protocol.

The simulated salivary fluid (SSF), gastric fluid (SGF), and intestinal fluid (SIF), prepared according to the INFOGEST protocol, contained physiologically relevant salt concentrations, in particular: SSF included KCl (15.1 mM), KH_2PO_4 (3.7 mM), $NaHCO_3$ (13.6 mM), $MgCl_2(H_2O)_6$ (0.15 mM), and $(NH_4)_2CO_3$ (0.06 mM); SGF contained KCl (6.9 mM), KH_2PO_4 (0.9 mM), $NaHCO_3$ (25 mM), NaCl (47.2 mM), $MgCl_2(H_2O)_6$ (0.1 mM), and $(NH_4)_2CO_3$ (0.5 mM); and SIF consisted of KCl (6.8 mM), KH_2PO_4 (0.8 mM), $NaHCO_3$ (85 mM), NaCl (38.4 mM), and $MgCl_2(H_2O)_6$ (0.33 mM). Stock solutions of salivary α-amylase (2505 U/mL), pepsin (60,180 U/mL) in water, and pancreatin (800 U/mL) and bile (134 mM) in SIF were freshly prepared just before the experiments.

Fresh apple pulp was ground with a meat grinder (7 mm-hole plate) to simulate oral processing.[38] Aliquots (10 g) of pulp or homogenate were mixed with α-amylase (75 U/mL). Subsequently, SSF and water were added at a 1:1 meal-to-fluid ratio (dry weight 13.5% for pulp, 10.4% for homogenate)[29] to obtain a 20 mL bolus, which was then incubated at 37 °C for 2 min at 15 rpm.

In the gastric phase, the bolus was combined with SGF and pepsin (2000 U/mL), and the pH was adjusted to 3 using 6 M HCl. The mixture was then diluted to a volume ratio of 1:1 (v/v) and incubated at 37 °C for 2 h at 15 rpm.

The intestinal phase was started by adding SIF, bile salts (10 mM), and pancreatin (100 U/mL), and adjusting the pH to 7 with 1 M NaOH, and the mixture was incubated at 37 °C for 2 h at 15 rpm.

Blank digestions were also performed in which the pulp or homogenate was replaced with water. After the intestinal phase, samples were centrifuged (30,000g, 4 °C, 70 min), and the supernatant, representing the bioaccessible fraction, was separated from the residue, representing the indigestible fraction.[39] The latter

https://doi.org/10.1021/acsfoodscitech.6c00023
ACS Food Sci. Technol. XXXX, XXX, XXX−XXX

was freeze-dried for WERP extraction; aliquots of ca. 10 mg of WERP were obtained. WERP from digested pulp and homogenate was designated as A_D and H_D, respectively (Figure S1).

A pectin-only model was also subjected to digestion, with the pectin fraction from apple pulp (A_U) suspended in water at a concentration of 2.8 mg/mL, to mimic the apple pectin concentration.[40]

2.4. Pectin Hydrolysis

The following general procedures were performed for sample hydrolysis. Freeze-dried WERP (2 mg) of each sample was dissolved in 2 mL of 0.1 M trifluoroacetic acid (TFA; Sigma-Aldrich, MO, USA) and hydrolyzed for 24 h at 80 °C.[41] After evaporation to dryness, the hydrolysates were analyzed for neutral sugar content by GC-FID after derivatization, as described in Section 2.5.2.[42] An additional 2 mg of each sample was hydrolyzed with 2 mL of 2 M TFA at 100 °C for 3 h. The solution was evaporated to dryness, then redissolved in Milli-Q water (2 mL), and treated with 110 μL of a 1:100 water-diluted solution of the pectinase enzyme (Sigma-Aldrich, MO, USA) for 1 h at 40 °C (pH 4) to cleave GalA residues from the backbone.[43,44] The commercial pectinase enzyme is an aqueous glycerol solution (2128 U/mL) derived from a selected strain of *Aspergillus niger*. According to the manufacturer, one unit of activity corresponds to the release of 1.0 μmol of GalA from polygalacturonic acid per minute at pH 4.0 and 25 °C. The released galacturonic acid was then quantified by the 3,5-dimethylphenol colorimetric assay,[45] as described in Section 2.5.1. This combined hydrolytic approach allowed the accurate quantification of both neutral sugars and uronic acids, overcoming the limitations of the individual methods.

2.5. Monomeric Composition

The monomeric composition was assessed by a spectrophotometric assay and gas chromatography using neutral monosaccharide standards (mannose, Man; xylose, Xyl; arabinose, Ara; rhamnose, Rha; glucose, Glc; galactose, Gal) and the galacturonic acid (GalA) standard (Sigma-Aldrich, MO, USA).

2.5.1. Spectrophotometric Assay. The standard of GalA and the residues recovered from the polysaccharide hydrolysis were quantified by an assay with the colorimetric reagent 3,5-dimethylphenol.[45]

An aliquot of 0.3 mL of the hydrolysate (diluted, if necessary, to contain between 25 and 100 μg of uronic acids per mL) was mixed with 0.3 mL of a mixture of sodium chloride and boric acid solution (prepared by adding 0.5 g of sodium chloride and 0.75 g of boric acid to 25 mL of water). 5 mL of concentrated sulfuric acid was added to the tube, which was then placed in a heating block at 70 °C while being agitated for 40 min. After the mixture was cooled, 0.2 mL of a 3,5-dimethylphenol solution (0.1 g in 100 mL of glacial acetic acid) was added and stirred immediately. The absorbance at 380 and 450 nm was measured using a UV−vis spectrophotometer Varian Cary 50 (Varian Inc., Palo Alto, CA, USA). The absorbance at 380 nm was subtracted from that at 450 nm for each sample. Using the absorbance values, the concentration of GalA in the various samples was determined using a previously constructed calibration curve.

2.5.2. Gas Chromatography. Neutral sugars (standards and the residues recovered from the polysaccharide hydrolysis) were derivatized by the following procedure.[42] The hydrolyzed solution was evaporated to dryness and dissolved in 1 mL of water; then, a freshly prepared solution of sodium tetrahydroborate in a 3 M ammonia (Prolabo, Paris, France) solution (100 mg/mL, 0.1 mL) was added. The mixture was kept at 40 °C for 1 h, and glacial acetic acid (0.1 mL, Sigma-Aldrich, Steinheim, Germany) was subsequently admixed. To a portion of the acidified solution (0.2 mL) were added *N*-methylimidazole (0.3 mL, Sigma-Aldrich, Steinheim, Germany) and acetic anhydride (2 mL, Sigma-Aldrich, Steinheim, Germany) and mixed. After the mixture was left for 10 min at 20 °C, water (5 mL) was supplemented, and when cooled, dichloromethane (1 mL, VWR, Fontenay-sous-Bois, France) was added. The solution was vigorously mixed on a vortex and then let to separate into two phases. The organic phase was then injected (1 μL) into the gas chromatograph (Trace 1300, Thermo Scientific, Milan, Italy) equipped with a fused silica capillary column with a 60 m × 0.32 mm internal diameter and 0.20 μm film thickness (SP 2330 Supelco), connected to an FID detector. The temperature ramp started from 220 to 250 °C (hold for 20 min) at 1 °C/min. The injector (split ratio 1:10) and the FID temperature were set at 300 °C. Helium, at a constant pressure of 70 kPa, was used as the carrier. Qualitative analysis was conducted by comparing the retention time of the peaks detected with those of commercial standards (Figure S2). For the quantitative analysis, calibration curves of all the neutral sugars were obtained, analyzing sugars standard solutions with concentrations ranging between 0.057 and 0.003 mg/mL.

2.6. Determination of Molecular Weights

The pectin molecular weight of the different samples was determined by SE-HPLC. The instrument was a binary pump Model LC 250 (PerkinElmer, Waltham, USA) equipped with a manual injection valve (type 7125 NS Rheo-dyne, Rohnert Park, CA, USA), a refractive index detector RID-10A (Shimadzu, Kyoto, Japan) and a UV detector Varian 2550 (Varian, Japan). The separation was carried out by combining the following two columns: an 8 μm, 300 × 7.5 mm, PL Aquagel-OH MIXED-H column (Agilent Technologies, Santa Clara, CA, USA) and a 250, 6 μm, 300 × 7.8 mm Ultrahydrogel column (Waters, Milford, MA, USA). The eluent was a solution of 0.2 M $NaNO_3$ in 0.01 M NaH_2PO_4 (pH 7.00). The separation was performed in isocratic mode at a flow rate of 0.7 mL/min, and the injection volume was 20 μL. Samples were prepared by dissolving 2 mg of polysaccharide in 1 mL of eluent, and the solution was filtered through a 0.22 μm nylon membrane before injection. A calibration curve obtained with standards of polyethylene glycol/poly(ethylene oxide) (PEG/PEO) of different molecular weights (range 106−1500, 000 g/mol, InfinityLab EasiVial, Agilent Technologies, Santa Clara, CA, USA) was used to estimate the pectin apparent molecular weight (aM_w, Figure S3).

2.7. NMR

NMR samples were prepared[46] by dissolving the isolated pectin (ca. 3 mg) in D_2O (0.6 mL; Sigma-Aldrich, Missouri, USA); the ^1H, ^{13}C, COSY, TOCSY, NOESY, HSQC-TOCSY, and $^1H-^{13}C$ HSQC spectra were acquired at 80, 40, and 25 °C by a Bruker Avance III 400 MHz digital NMR spectrometer (Bruker, Karlsruhe, Germany). The Bruker noesygppr1d sequence was used to acquire 1D ^1H spectra suppressing the solvent. DSS was used as an external standard for the ^1H and ^{13}C reference. The following Bruker pulse sequences and parameters were used to acquire the spectra. ^{13}C: DEPT135 (Bruker pulse program, Bpp: deptsp135), scan number (NS) = 20864, experimental time (t_{exp}) ca. 25 h; COSY (Bpp: cosygpprqf): TD in F1 = 360, TD F2 = 2k, NS = 84, Non Uniform Sampling (NUS) = 50%, t_{exp} = 14 h; $^1H-^{13}C$ HSQC (Bpp: hsqcetgpprsisp2.2), TD in F1 = 432, TD F2 = 1.5k, NS = 204, t_{exp} = 32 h; NOESY (Bpp: noesyphpr): TD in F1 = 384, TD F2 = 2k, NS = 80, NUS = 50%, t_{exp} = 11 h; mixing time 200 and 600 ms.; TOCSY (Bpp: mlevphpr.2): time domain (TD) in F1 = 320, TD F2 = 2k, NS = 80, t_{exp} = 16 h; mixing time 65 ms; HSQC-TOCSY (Bpp: hsqcdietgpsisp.2) TD in F1 = 512, TD F2 = 2k, NS = 96, NUS = 50%, t_{exp} = 16 h; mixing time 65 ms.

2.8. In Situ NMR Experiment

The capacity of α-arabinofuranosidase (α-AF) to remove arabinose from pectin under gastric digestive conditions was ascertained by in situ NMR experiments.

To this purpose, two samples were prepared. The first sample consisted of 4 mg of A_U suspended in 0.479 mL of water and added with 6 M HCl until pH 5, representing the pH recommended by the producer for testing α-AF. Immediately before the start of the NMR experiment, 15.4 μL of α-AF (300 U/mL, Megazyme, GH51, Wicklow, Ireland) was added to this solution together with an appropriate volume of D_2O to reach a final volume of 0.6 mL. The solution obtained was immediately inserted into an NMR tube, and the experiment started.

The second sample aimed at resembling the simulated gastrointestinal conditions under which α-AF and pectin were exposed during in vitro digestion. To this purpose, 4 mg of A_U was added with

https://doi.org/10.1021/acsfoodscitech.6c00023
ACS Food Sci. Technol. XXXX, XXX, XXX−XXX

Table 1. Monomeric Composition Determined by GC and Spectrophotometry and Expressed in Terms of % w/w of Total Identified Monomers in the WERP Fraction Isolated from Undigested Apple (A_U), Undigested Homogenate (H_U), Digested Apple (A_D), and Digested Homogenate (H_D)[a]

	monomeric composition (% w/w of total identified monomers)						
	Ara	Gal	Rha	Glc	Man	Xyl	GalA
A_U	48.9 (1.1)[a]	14.5 (0.9)[a]	5.9 (3.2)[a]	10.3 (0.4)[a]	0.3 (0.1)[a]	0.5 (0.1)[a]	19.5 (0.8)[b]
H_U	48.3 (3.7)[a]	15.6 (1.5)[ab]	6.7 (1.0)[a]	9.9 (1.6)[a]	1.4 (0.1)[a]	0.6 (0.1)[a]	17.4 (1.5)[ab]
A_D	10.5 (0.2)[b]	20.8 (1.8)[b]	2.8 (1.1)[a]	9.5 (1.0)[a]	6.6 (0.9)[b]	0.6 (0.1)[a]	49.1 (3.3)[c]
H_D	45.6 (0.4)[a]	26.7 (1.5)[c]	4.6 (1.4)[a]	6.0 (1.1)[a]	4.4 (0.8)[b]	1.0 (0.1)[a]	11.7 (0.5)[a]

[a]Results are expressed as "mean (standard deviation)" of at least three measurements on two replicated samples. [a,b,c]: in the same column, means indicated by different letters are significantly different ($p < 0.05$).

Table 2. ^{1}H and ^{13}C Chemical Shifts (ppm) of Assigned Residues[a]

	H-1	H-2	H-3	H-4	H-5	H-6
residue	C-1	C-2	C-3	C-4	C-5	C-6
α-1,3,5-Araf_1	5.11	4.08	4.00	3.92	3.8/3.69	
	110	84	80	79.85	64.4	
α-1,5-Araf_1	5.06	4.24	4.05	3.87	3.69	
	110.6	82.3	78[b]	83	65	
α-1,5-Araf_2	5.03	4.1	4.07	3.96	3.83/3.77	
	110.7	83.7	77[b]	n.d.	65	
α-1,4-Gal*p*A	5.06	3.72	3.96	4.42	n.d.	
	102.6	70	71	80	n.d.	
α-1,4-Gal*p*A	4.92	3.7	3.94	4.4	n.d.	
	103	70.9	71.2	80	n.d.	
α-1,?-Rha	4.96	3.83	3.7	3.38	3.88	1.24
	102.5	72−70	72−70	73	71.6	18.7
β-1,?-Gal*p*	4.57	4.096	3.72	3.65	n.d.	n.d.
	107.4	n.d.	71.4	n.d.	n.d.	n.d.

[a]Experiments were conducted at 80 °C unless otherwise stated. Not determined (n.d.); uncertainty in assignment (?). [b]25 °C.

0.479 mL of SGF, 0.3 μL of $CaCl_2$ (44.103 g/L), and 40 μL of pepsin (60, 180 U/mL), and the solution was adjusted to pH 3 with 6 M HCl. Immediately before the NMR experiment, 15.4 μL of α-AF was added together with an appropriate quantity of D_2O to reach a volume of 0.6 mL. The final solution was immediately transferred to an NMR tube, and the experiment started.

NMR experiments were conducted at 37 °C for a maximum of 120 min, with ^{1}H spectra recorded every 30 min. The Ara peaks, resonating between 5.15 and 5.03 ppm, were integrated and summed. The removal of Ara from the polysaccharide was assessed by monitoring the variation of the I/I_0 values throughout the reaction time (min): I_0 representing the integral of the Ara signals at time $t = 0$ min and I representing the integral of the same signals at time t.

2.9. Statistical Analysis

Results are expressed as "mean (standard deviation)" of at least three measurements on two replicated samples. The homogeneity of variance was checked by Bartlett's test, and statistically significant differences among means ($p < 0.05$) were assessed by the t-test or one-way ANOVA followed by the Tukey test, using R software (v. 4.4.1) for Windows (The R foundation for statistical computing, 2024).

3. RESULTS AND DISCUSSION

3.1. Chemical Characterization of WERP from Apple Pulp and Homogenate

WERP extracted from undigested apple pulp (A_U) and undigested homogenate (H_U) was first characterized to define their structural features and to assess whether processing affected their molecular architecture prior to digestion. To this end, the neutral sugar composition was determined by GC after controlled hydrolysis of the polymers. A first hydrolysis step was performed under mild acidic conditions (0.1 M TFA, 80 °C, 24 h) to minimize arabinose degradation and enable reliable quantification of neutral sugars released from the polysaccharide matrix. This approach is particularly suitable for Ara-rich side chains, which are prone to decomposition under harsher conditions.[41]

To maximize GalA recovery from the backbone, a stronger hydrolysis was conducted (2 M TFA, 100 °C, 3 h), followed by an additional enzymatic depolymerization step.[43,44] GalA was then quantified by a conventional colorimetric method. The resulting monomer profiles are summarized in Table 1 as % w/w of total identified monomers in A_U and H_U. As expected for an extraction obtained under mild conditions, WERP from both A_U and H_U was characterized by a significant amount of neutral sugars, particularly arabinose (Table 1). Overall, A_U and H_U displayed comparable profiles, with high Ara concentrations (ca. 50%), along with Gal concentrations (ca. 15%) and GalA concentrations (ca. 20%). This composition is consistent with an RG-I-enriched pectic fraction, characterized by abundant neutral side chains relative to the GalA-rich HG domain.

Because the HG/RG-I balance in extracted pectic materials is strongly influenced by extraction strategy,[47] the GalA range observed here is in line with the preferential recovery of RG-I-rich populations under mild conditions. Acid-based methods typically yield HG-rich pectins with high GalA contents (>65%) but may promote degradation of neutral sugar side chains, whereas mild or nonacidic extractions preferentially recover RG-I-rich polymers with lower GalA and higher Ara/Gal.[48,49] In line with this, GalA contents in the 20−30% range

https://doi.org/10.1021/acsfoodscitech.6c00023
ACS Food Sci. Technol. XXXX, XXX, XXX−XXX

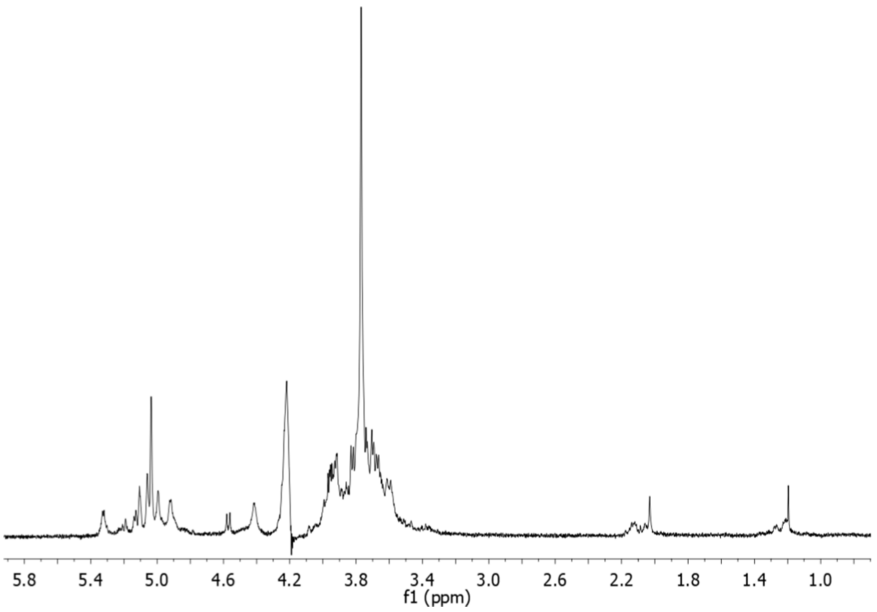

Figure 1. ^{1}H NMR spectrum of pectin extracted from apple homogenate (H_U, undigested). The spectrum was acquired at 80 °C, suppressing the solvent (D_2O, residual signal at ca. 4.2 ppm). Sodium trimethylsilylpropanesulfonate (DSS) was used as the external standard. The horizontal axis (f1) reports a ^{1}H chemical shift (ppm).

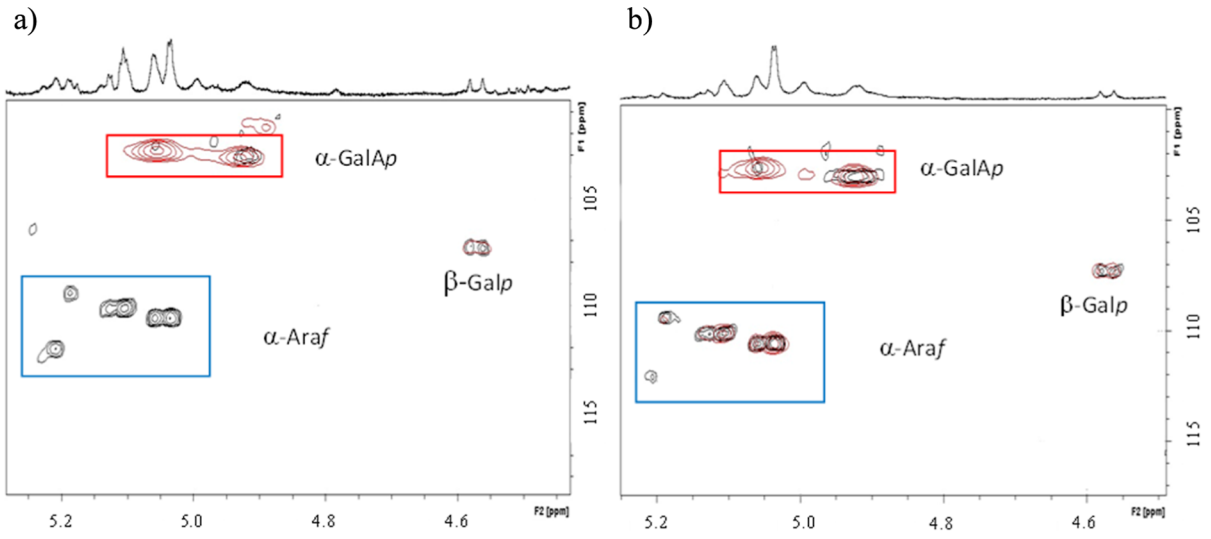

Figure 2. ^{1}H−^{13}C HSQC WERP's spectra of a) undigested apple (A_U, black), digested apple (A_D, red), and b) undigested homogenate (H_U, black), digested homogenate (H_D, red) recorded at 80 °C. Detail of the anomeric region. Corresponding ^{1}H spectra of undigested samples are reported as horizontal traces. The horizontal axis ($f2$) reports the ^{1}H chemical shift (ppm); the vertical axis ($f1$) reports the ^{13}C chemical shift (ppm). *α*-GalA*p*: galacturonic acid, *α*-pyranoside; *α*-Ara*f*: arabinose, *α*-furanoside; *β*-Gal*p*: galactose, *β*-pyranoside. The boxes group the signals assigned to the indicated residues.

have been reported for mildly extracted pectins from pumpkin[50] and citrus[51] and for RG-I-enriched apple pectins obtained after malic acid extraction.[52]

Similarly, water-extracted okra pectins contain higher proportions of RG-I compared with acid- or alkali-extracted counterparts.[53] High Ara levels also favor the recovery of WERP because arabinan-rich RG-I side chains increase hydration and molecular mobility, thereby enhancing water affinity and solubility.[11,54] Consistent with this rationale, the mild, nonacidic conditions applied here likely contributed to preserving Ara-rich side chains in both A_U and H_U.

While A_U and H_U displayed similar monosaccharide compositions, compositional similarity alone does not guarantee comparable architecture. Therefore, 1D and 2D NMR analyses were performed to assess domain integrity and the organization of key residues. Signal assignments are summarized in Table 2.

In the ^{1}H NMR spectra of both A_U and H_U, anomeric protons appeared between 4.47 and 5.20 ppm, whereas non-anomeric resonances largely overlapped between 3.2 and 4.0 ppm, consistent with complex pectic polysaccharides.

The methyl protons of esterified GalA units were observed as prominent singlets at 3.77 ppm. In addition, signals from Rha $-CH_3$ groups and GalA acetyl derivatives were detected at a high field (around 1.17 and 2.0 ppm, respectively) (Figure 1).

https://doi.org/10.1021/acsfoodscitech.6c00023
ACS Food Sci. Technol. XXXX, XXX, XXX−XXX

A broad resonance at 5.32 ppm was detected in both A_U and H_U. Based on TOCSY/COSY/HSQC features, this signal was assigned to starch, with the characteristic correlations at H-1/C-1 = 5.32/102.8 ppm; H-2/C-2 = 3.6/74.7 ppm; H-3/C-3 = 3.9/76.3 ppm; H-4/C-4 = 3.8/79.7 ppm; H-5/C-5 not determined; and H-6/C-6 = 3.7−3.8/64.6 ppm (Figure S4), in agreement with literature assignments.[55] The presence of starch was additionally supported by the Lugol test (Figure S5). Because the ^{1}H spectra of pectic polysaccharides are highly congested, structural comparison between A_U and H_U was primarily based on ^{1}H−^{13}C HSQC fingerprints (Figure 2). In particular, the ^{1}H−^{13}C HSQC anomeric region of A_U and H_U was dominated by clusters of correlations attributable to arabinofuranosyl residues, in excellent agreement with published assignments for RG-I arabinans.[56−59] As expected, distinct signals corresponding to terminal, linear, and branching arabinose units could be resolved in the anomeric region, reflecting the structural heterogeneity of arabinan side chains.

Specifically, the H-1/C-1 correlations at 5.18/109.7 and 5.20/112 ppm were consistent with terminal Ara residues,[56] whereas the signal at 5.11/110 ppm was assigned to a branching-point Ara unit. This assignment is supported by ^{13}C chemical shifts consistent with a furanose residue substituted at positions 1, 3, and 5 (Table 2).[60] A closely related anomeric HSQC cross-peak at 5.12/110 ppm showed a TOCSY spin system similar to that of the 5.11/110 ppm signal and was therefore interpreted as a branching Ara unit in a slightly different local chemical environment.[61,62]

Signals at 5.06/110.6 and 5.03/110.7 ppm were assigned to linear Ara units (Table 2). In addition, GalA and Rha anomeric resonances were identified (e.g., GalA H-1/C-1 at 4.92/103 ppm with the associated H-5/C-5 correlation at 5.03/73 ppm; Figure S6),[37,63,64] together with α-Rha signals (4.96/102.5 ppm)[65] and β-Gal*p* residues at 4.57/107.4 at 80 °C.[66]

Crucially, a comparison of HSQC and TOCSY spectra showed that A_U and H_U exhibited nearly identical patterns in the anomeric region, particularly for the arabinose clusters (Figure 2). The close correspondence of signals attributed to terminal units, linear side chains, and branching points indicates that the key structural motifs of the RG-I arabinan side chains were preserved in H_U. Accordingly, the applied technological processing revealed no detectable alterations in the RG-I arabinan architecture within the resolution of the applied NMR approach prior to digestion. A putative structure consistent with these features is illustrated in Figure S7a.

To complement the compositional and NMR evidence, A_U and H_U were compared in terms of molecular weight distribution to further assess whether WERP from the two matrices exhibited comparable polymer size profiles before digestion. SE-HPLC profiles indicated highly similar elution patterns for the undigested samples, with closely matching aM_w values (Figure 3). The aM_w values were 2.5×10^5 g/mol for A_U and 2.43×10^5 g/mol for H_U. Taken together, GC composition, NMR fingerprints, and SE-HPLC profiles consistently indicate no detectable processing-related changes in WERP prior to digestion under the conditions used to obtain the homogenate (blanching/pasteurization and high-pressure homogenization) despite the associated tissue disruption.

These findings differ from previous reports[67] describing substantial Ara loss and pectin depolymerization after thermal processing, underscoring that processing effects on pectin depend on cultivar, ripening stage, and processing severity.[68−70] For example, loss of neutral sugar branches was observed in apple purée obtained by thermal treatments and HPH from freshly harvested apples, whereas the same process did not induce detectable structural changes in six-month-old apples,[49] highlighting the interplay of biological and technological factors beyond chemical degradation alone.

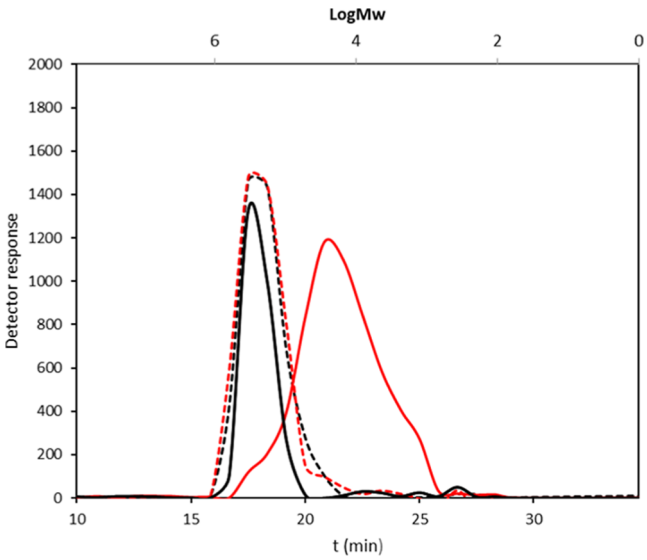

Figure 3. SE-HPLC elution patterns of WERP of undigested apple (A_U, black solid trace), digested apple (A_D, red solid trace), undigested homogenate (H_U, black dotted trace), and digested homogenate (H_D, red dotted trace). The logarithm of PEG/PEO standards' molecular weights (in g/mol) is indicated.

3.2. Chemical Characterization of WERP from Digested Apple Pulp and Homogenate

Monomeric profiling of the digested samples revealed a clear divergence between the two matrices (Table 1). In digested apple pulp (A_D), arabinose decreased sharply, whereas the digested homogenate (H_D) showed comparatively limited compositional variation. At the same time, compositional data in digested samples should be interpreted with care because pancreatin used in the intestinal phase introduced lactose (Figure S8), which could contribute to the GC-derived Gal (and partly Glc) signal. Accordingly, the GC-derived Gal reflects the overall galactose released from all galactose-containing species present in the sample. In this context, NMR provides an orthogonal, structure-resolved readout that distinguishes pectic Gal from other galactose sources (Figure S9) while also providing pectin-specific structural markers in the presence of non-pectic carbohydrate contributions, enabling the fate of pectic structural units to be interpreted alongside RG-I fingerprints.

Consistent with the compositional trends, NMR spectroscopy provided direct evidence of matrix-dependent structural changes. In the ^{1}H−^{13}C HSQC spectra, the cluster of arabinose anomeric correlations observed in the undigested samples was no longer detectable in A_D (Figure 2a). In contrast, GalA correlations (5.06/102.6 and 4.92/103 ppm) and the galactose signal (4.57/107.4 ppm) remained detectable in the digested samples (Figure 2). Taken together, the loss of arabinan-specific correlations and the retained GalA/Gal signals indicate that WERP isolated from digested apple pulp underwent substantial modification, dominated by

https://doi.org/10.1021/acsfoodscitech.6c00023
ACS Food Sci. Technol. XXXX, XXX, XXX−XXX

the depletion of arabinose-rich RG-I side chains and a shift toward a less branched architecture. By comparison, H_D retained the overall anomeric fingerprint, with only modest changes in arabinan-related features, consistent with limited modification of the RG-I side-chain motifs under these conditions.

Moreover, the $^{1}H-^{13}C$ HSQC spectrum of the WERP filtrate showed a set of anomeric correlations (5.11/106.2, 5.10/105.7, and 5.09/105.3 ppm) consistent with arabinose oligomers previously reported in the literature.[71] GalA correlations were not detected in this fraction, which is compatible with these low-molecular-weight species being predominantly arabinan-derived rather than GalA-containing backbone fragments and provides additional, albeit qualitative, support for RG-I side-chain debranching. To assess the extent of size changes accompanying these structural transformations, the molecular weight distribution of digested WERP fractions was examined by SE-HPLC (Figure 3). A_D exhibited a highly dispersed profile consisting of three components. Only a minor fraction eluted at molecular weight comparable to native WERP, whereas the dominant component corresponded to an aM_w of 2.5×10^4 g/mol, i.e., roughly an order of magnitude lower than A_U. A further fraction at a lower aM_w was also detected.

Overall, the combined GC/NMR/SE-HPLC evidence indicates that the digestion of apple pulp is associated with pronounced size reduction and compositional simplification of the RG-I-rich WERP fraction. The ca. 10-fold decrease in aM_w is most consistently explained by extensive removal of arabinose-rich side chains, which would compact the polymer and reduce its hydrodynamic volume. This interpretation is aligned with the strong depletion of Ara and the concurrent relative enrichment in GalA observed for A_D (Table 1), whereas a scenario dominated by extensive fragmentation of the GalA-rich HG backbone would not necessarily be expected to yield such a compositional shift in the recovered WERP fraction. Nevertheless, while arabinose side-chain loss remains the main mechanistic pathway supported by our data, a limited contribution from minor HG backbone cleavage cannot be excluded; accordingly, A_D-derived WERP is expected to reach the large intestine as a mixture of depolymerization products (Figure S7b). In contrast, no comparable structural changes were observed for H_D. The SE-HPLC profile remained dominated by a polymeric peak with an aM_w close to that of H_U (2.3×10^5 g/mol, Figure 3), and the HSQC anomeric region retained the characteristic RG-I arabinan features (Figure 2b). The pronounced A_D-H_D divergence therefore indicates that the structural fate of RG-I-rich pectins during digestion is strongly dependent on the processing history of the apple matrix.

3.3. Chemical Characterization of Digested Apple Model Pectin

The pronounced divergence between digested apple pulp and the homogenate raised the question of whether the gastrointestinal environment alone could account for the modifications detected in the RG-I-rich fraction. To address this point, isolated apple pectin was subjected to the same in vitro digestion protocol used for the food matrices, and its structural features were monitored by NMR throughout the gastric and intestinal phases.

Across digestion, the isolated pectin showed no detectable changes in its NMR fingerprints, consistent with previous studies using standardized models (including INFOGEST) that reported minimal or no modification of purified citrus and apple pectins under simulated gastrointestinal conditions.[3,22] Likewise, in situ NMR confirmed that the applied digestion conditions did not produce detectable alterations of the polysaccharide structure (Figure S8). Also, the methyl-ester signal of GalA residues remained essentially unchanged (Figure S10), in agreement with reports, indicating that only limited de-esterification/deacetylation occurs under mildly acidic gastric conditions.[3] Furthermore, arabinose release from pectic polysaccharides has been reported to require more severe acidity (pH 1−2) and to be strongly inhibited at pH values around 3, corresponding to the gastric conditions applied here.[72]

Taken together, these observations indicate that digestive fluids and digestive enzymes, acting on isolated pectin, are insufficient to reproduce the extensive arabinose side-chain loss and concomitant size reduction observed in digested apple pulp. The absence of comparable modifications in the isolated-pH/enzyme control therefore points to additional matrix-associated contributions present in apple tissue.

A mechanistically plausible scenario is the involvement of endogenous apple enzymes that selectively target RG-I side chains under gastrointestinal-like conditions. Among the candidates, α-L-arabinofuranosidase (AF), one of the major cell-wall glycosidase implicated in arabinosyl residue removal and showing pronounced post-harvest regulation in Golden Delicious, particularly at early storage stages,[73,74] would be compatible with the selective depletion of arabinose observed in A_D. Importantly, fresh apple pulp did not undergo processing steps expected to inactivate endogenous enzymes prior to digestion, allowing such activities to potentially persist in the gastric phase. Reported AF activity ranges are compatible with gastric-like temperature and pH, and divalent cations (e.g., Ca^{2+}) present in digestive fluids may further support activity.[75] Although proteolysis during digestion can partially cleave AF, residual activity toward arabinose-containing substrates has been described.[76,77]

To evaluate the compatibility of this hypothesis with our observations, in situ NMR experiments were performed under gastric-like conditions using A_U supplemented with a commercial AF. A time-dependent decrease in arabinose signal integrals was observed at both pH 5 and at pH 3 in the simulated gastric fluid containing pepsin, with a more pronounced effect under gastric conditions. While these experiments do not establish the in vivo contribution of endogenous AF and have to be considered preliminary, they indicate that arabinose side-chain cleavage is feasible under digestion-relevant conditions, even in the presence of proteolytic activity. Comparable persistence of plant enzymes under digestive conditions has been reported in other fruit systems, including polygalacturonases from tomato[78] and proteases such as actinidin (kiwifruit) and bromelain (pineapple), which retain activity across broad pH ranges and in the presence of gastric enzymes.[79,80]

This framework also provides a coherent rationale for the contrasting behavior of the processed homogenate. Thermal and mechanical treatments associated with homogenization are known to reduce or inactivate AF activity.[34,81] In addition, extensive matrix disruption may facilitate exposure to digestive proteolysis, further disfavoring the persistence of any residual endogenous pectinolytic activities. Accordingly, the pectic

https://doi.org/10.1021/acsfoodscitech.6c00023
ACS Food Sci. Technol. XXXX, XXX, XXX−XXX

fraction associated with homogenized apples remains largely structurally intact during digestion.

Collectively, our results show that processing can switch the post-digestive structural form of apple pectin by altering the matrix context in which digestion occurs. Under standardized INFOGEST conditions, the RG-I-enriched WERP fraction recovered from intact apple pulp underwent pronounced depletion of arabinose-rich side chains accompanied by a marked reduction in aM_w, whereas WERP recovered from processed homogenate largely retained its pre-digestive RG-I fingerprint. Digestion of isolated apple pectin under the same protocol did not reproduce these transformations, indicating that the gastrointestinal environment alone is insufficient and supporting a matrix-dependent contribution that is attenuated by thermal/mechanical processing. Previous work on apple homogenate[29] obtained under comparable processing conditions showed extensive tissue disruption after homogenization; therefore, the fact that the strongest RG-I remodeling was observed here in the more intact pulp indicates that matrix disintegration alone is insufficient to explain the different digestion outcomes. While the mechanistic basis of this matrix effect, including the possible contribution of tissue-associated enzymatic activities, remains to be established and represents an important limitation of the present study, the present findings caution against extrapolating the digestive fate of pectin from purified substrates to fruit tissues and identify matrix processing state as a key variable shaping the post-digestive molecular architecture of pectin. Direct enzyme-focused studies under digestion-relevant conditions are required to test this mechanistic hypothesis. Future mechanistic studies should also include step-resolved structural analysis after SGF and SIF in order to identify more precisely the stage at which the observed remodeling occurs.

■ ASSOCIATED CONTENT

Supporting Information

The Supporting Information is available free of charge at https://pubs.acs.org/doi/10.1021/acsfoodscitech.6c00023.

Graphical summary of sample preparation and digestion workflow (Figure S1); GC chromatograms of neutral sugars (Figure S2); SE-HPLC chromatograms and calibration with PEG/PEO standards (Figure S3); additional NMR spectra (^{1}H, ^{1}H−^{13}C HSQC, TOCSY) for H_U and A_D (Figures S4 and S6); Lugol's iodine test for starch (Figure S5); putative structure of WERP (Figure S7); in situ NMR digestion of model pectin (Figure S8); HSQC comparison of A_D with lactose and glucose standards (Figure S9); and additional NMR spectra for model pectin before and after digestion (Figure S10) (PDF)

■ AUTHOR INFORMATION

Corresponding Author

Clara Comuzzi − *Department of Agricultural, Food, Environmental and Animal Sciences, University of Udine, I-33100 Udine, Italy*; orcid.org/0000-0002-6137-9478; Phone: +390432558845; Email: clara.comuzzi@uniud.it

Authors

Marilisa Alongi − *Department of Agricultural, Food, Environmental and Animal Sciences, University of Udine, I-33100 Udine, Italy*

Umberto Lanza − *Department of Agricultural, Food, Environmental and Animal Sciences, University of Udine, I-33100 Udine, Italy*

Asja Brovedani − *Department of Agricultural, Food, Environmental and Animal Sciences, University of Udine, I-33100 Udine, Italy*

Erica Moret − *Department of Agricultural, Food, Environmental and Animal Sciences, University of Udine, I-33100 Udine, Italy*; orcid.org/0000-0001-6873-1350

Lara Manzocco − *Department of Agricultural, Food, Environmental and Animal Sciences, University of Udine, I-33100 Udine, Italy*

Maria Cristina Nicoli − *Department of Agricultural, Food, Environmental and Animal Sciences, University of Udine, I-33100 Udine, Italy*

Complete contact information is available at: https://pubs.acs.org/10.1021/acsfoodscitech.6c00023

Author Contributions

Designed the experiments: C.C., M.A., U.L., A.B., E.M., L.M., and M.C.N. Methodology: C.C., M.A., U.L., A.B., E.M., L.M., and M.C.N. Conducted the experiments: C.C., M.A., U.L., A.B., and E.M. Analyzed the data: C.C., M.A., U.L., A.B., E.M., L.M., and M.C.N. Discussed the results: C.C., M.A., U.L., A.B., E.M., L.M., and M.C.N. Wrote the manuscript: C.C., M.A., U.L., A.B., E.M., L.M., and M.C.N. Discussed and revised the manuscript: C.C., M.A., U.L., A.B., E.M., L.M., and M.C.N. All authors read and approved the final manuscript.

Notes

Declaration of generative AI and AI-assisted technologies in the writing process: During the preparation of this work, the authors used Grammarly in order to improve the language and the readability of the manuscript. After using this tool, the authors reviewed and edited the content as needed and took full responsibility for the content of the publication.
The authors declare no competing financial interest.

■ ACKNOWLEDGMENTS

This research was carried out within the interdisciplinary research project of the University of Udine, "Il tempo della mela—TEAM," supported by Fondazione Friuli. The authors thank Dr. Paolo Martinuzzi for contributing to NMR measurements and Dr. Antonino Crivello for performing the in situ NMR experiments.

■ ABBREVIATIONS USED

A_D, digested apple pulp; AF, α-arabinofuranosidase; aM_w, apparent weight-average molecular weight; A_U, undigested apple pulp; COSY, correlation spectroscopy; DSS, 4,4-dimethyl-4-silapentane-1-sulfonic acid; D_2O, deuterium oxide; EtOH, ethanol; GalA, galacturonic acid; GC-FID, gas chromatography−flame ionization detection; H_D, digested apple homogenate; HSQC, heteronuclear single quantum coherence; H_U, undigested apple homogenate; INFOGEST, standardized in vitro digestion protocol; NMR, nuclear magnetic resonance; PEG, polyethylene glycol; PEO, poly(ethylene oxide); RG-I, rhamnogalacturonan I; SE-HPLC, size-exclusion high-performance liquid chromatography; SGF, simulated gastric fluid; SIF, simulated intestinal fluid; SSF, simulated salivary fluid; TFA, trifluoroacetic acid; TOCSY,

https://doi.org/10.1021/acsfoodscitech.6c00023
ACS Food Sci. Technol. XXXX, XXX, XXX−XXX

total correlation spectroscopy; WERP, water-extracted RG-I-enriched pectin fraction.

REFERENCES

(1) Del Rio, D.; Rodriguez-Mateos, A.; Spencer, J. P. E.; Tognolini, M.; Borges, G.; Crozier, A. Dietary (Poly)Phenolics in Human Health: Structures, Bioavailability, and Evidence of Protective Effects against Chronic Diseases. *Antioxid. Redox Signaling* **2013**, *18* (14), 1818−1892.

(2) Slavin, J. Fiber and Prebiotics: Mechanisms and Health Benefits. *Nutrients* **2013**, *5* (4), 1417−1435.

(3) Capuano, E. The Behavior of Dietary Fiber in the Gastrointestinal Tract Determines Its Physiological Effect. *Crit. Rev. Food Sci. Nutr.* **2017**, *57* (16), 3543−3564.

(4) Holscher, H. D. Dietary Fiber and Prebiotics and the Gastrointestinal Microbiota. *Gut Microbes* **2017**, *8* (2), 172−184.

(5) McRorie, J. W.; McKeown, N. M. Understanding the Physics of Functional Fibers in the Gastrointestinal Tract: An Evidence-Based Approach to Resolving Enduring Misconceptions about Insoluble and Soluble Fiber. *J. Acad. Nutr. Diet.* **2017**, *117* (2), 251−264.

(6) Padayachee, A.; Day, L.; Howell, K.; Gidley, M. J. Complexity and Health Functionality of Plant Cell Wall Fibers from Fruits and Vegetables. *Crit. Rev. Food Sci. Nutr.* **2017**, *57* (1), 59−81.

(7) Du, J.; Anderson, C. T.; Xiao, C. Dynamics of Pectic Homogalacturonan in Cellular Morphogenesis and Adhesion, Wall Integrity Sensing and Plant Development. *Nat. Plants* **2022**, *8* (4), 332−340.

(8) Du, J.; Kirui, A.; Huang, S.; Wang, L.; Barnes, W. J.; Kiemle, S. N.; Zheng, Y.; Rui, Y.; Ruan, M.; Qi, S.; Kim, S. H.; Wang, T.; Cosgrove, D. J.; Anderson, C. T.; Xiao, C. Mutations in the Pectin Methyltransferase QUASIMODO2 Influence Cellulose Biosynthesis and Wall Integrity in Arabidopsis. *Plant Cell* **2020**, *32* (11), 3576−3597.

(9) Kirui, A.; Du, J.; Zhao, W.; Barnes, W.; Kang, X.; Anderson, C. T.; Xiao, C.; Wang, T. A Pectin Methyltransferase Modulates Polysaccharide Dynamics and Interactions in Arabidopsis Primary Cell Walls: Evidence from Solid-State NMR. *Carbohydr. Polym.* **2021**, *270*, 118370.

(10) Ng, J. K. T.; Zujovic, Z. D.; Smith, B. G.; Johnston, J. W.; Schröder, R.; Melton, L. D. Solid-State 13C NMR Study of the Mobility of Polysaccharides in the Cell Walls of Two Apple Cultivars of Different Firmness. *Carbohydr. Res.* **2014**, *386* (1), 1−6.

(11) Kaczmarska, A.; Pieczywek, P. M.; Cybulska, J.; Zdunek, A. Structure and Functionality of Rhamnogalacturonan I in the Cell Wall and in Solution: A Review. *Carbohydr. Polym.* **2022**, *278*, 118909.

(12) Beukema, M.; Faas, M. M.; de Vos, P. The Effects of Different Dietary Fiber Pectin Structures on the Gastrointestinal Immune Barrier: Impact via Gut Microbiota and Direct Effects on Immune Cells. *Exp. Mol. Med.* **2020**, *52* (9), 1364−1376.

(13) Calvete-Torre, I.; Sabater, C.; Antón, M. J.; Moreno, F. J.; Riestra, S.; Margolles, A.; Ruiz, L. Prebiotic Potential of Apple Pomace and Pectins from Different Apple Varieties: Modulatory Effects on Key Target Commensal Microbial Populations. *Food Hydrocoll.* **2022**, *133*, 107958.

(14) Van den Abbeele, P.; Deyaert, S.; Albers, R.; Baudot, A.; Mercenier, A.; Carrot, R. G.-I. Reduces Interindividual Differences between 24 Adults through Consistent Effects on Gut Microbiota Composition and Function Ex Vivo. *Nutrients* **2023**, *15* (9), 2090.

(15) Zhang, J.; Sun, Z.; Cheng, L.; Kang, J.; Liu, Y.; Zhao, Y.; Xiao, M.; Liu, H.; Zhu, Q.; Guo, Q.; Lin, C. Structural Characterization of Water-Soluble Pectin from the Fruit of Diospyros Lotus L. and Its Protective Effects against DSS-Induced Colitis in Mice. *J. Agric. Food Chem.* **2025**, *73* (2), 1630−1641.

(16) Van den Abbeele, P.; Duysburgh, C.; Cleenwerck, I.; Albers, R.; Marzorati, M.; Mercenier, A. Consistent Prebiotic Effects of Carrot Rg-i on the Gut Microbiota of Four Human Adult Donors in the Shime® Model despite Baseline Individual Variability. *Microorganisms* **2021**, *9* (10), 2142.

(17) Jiang, S.; Lu, C.; Zhao, C.; Yuan, F.; Jin, J.; Wang, Y.; Wang, X.; Yan, T.; Gao, T. Pectin Polysaccharides from Cascara Prevent Metabolic Dysfunction-Associated Fatty Liver Disease Development by Regulating Gut Microbiota and Liver Metabolism. *J. Agric. Food Chem.* **2025**, *73* (51), 32650−32660.

(18) Gu, J.; Lin, L.; Zhao, M. Highly Branched Rhamnogalacturonan-I Type Pectin from Wolfberry: Purification, Characterization, and Structure-Prebiotic/Immunomodulatory Activity Relationship. *J. Agric. Food Chem.* **2024**, *72* (24), 14022−14034.

(19) Yüksel, E.; Voragen, A. G. J.; Kort, R. The Pectin Metabolizing Capacity of the Human Gut Microbiota. *Crit. Rev. Food Sci. Nutr.* **2025**, *65* (25), 4823−4845.

(20) Dávila León, R.; González-Vázquez, M.; Lima-Villegas, K. E.; Mora-Escobedo, R.; Calderón-Domínguez, G. In Vitro Gastrointestinal Digestion Methods of Carbohydrate-Rich Foods. *Food Sci. Nutr.* **2024**, *12* (2), 722−733.

(21) Torp Nielsen, M.; Roman, L.; Corredig, M. In Vitro Gastric Digestion of Polysaccharides in Mixed Dispersions: Evaluating the Contribution of Human Salivary α-Amylase on Starch Molecular Breakdown. *Curr. Res. Food Sci.* **2024**, *8*, 100759.

(22) Gallego-Lobillo, P.; Ferreira-Lazarte, A.; Hernández-Hernández, O.; Villamiel, M. In Vitro Digestion of Polysaccharides: InfoGest Protocol and Use of Small Intestinal Extract from Rat. *Food Res. Int.* **2021**, *140*, 110054.

(23) Cao, W.; Guan, S.; Yuan, Y.; Wang, Y.; Mst Nushrat, Y.; Liu, Y.; Tong, Y.; Yu, S.; Hua, X. The Digestive Behavior of Pectin in Human Gastrointestinal Tract: A Review on Fermentation Characteristics and Degradation Mechanism. *Crit. Rev. Food Sci. Nutr.* **2024**, *64* (33), 12500−12523.

(24) Lopez-Rodulfo, I. M.; Stentoft, E. W.; Martinez, M. M. Comparative Assessment of Polyphenol Bioaccessibility in Cold-Pressed Apple Fractions Using Static and Semi-Dynamic Digestion Models. *Food Res. Int.* **2025**, *202*, 115743.

(25) Lopez-Rodulfo, I. M.; Tsochatzis, E. D.; Stentoft, E. W.; Martinez-Carrasco, P.; Bechtner, J. D.; Martinez, M. M. Partitioning and in Vitro Bioaccessibility of Apple Polyphenols during Mechanical and Physiological Extraction: A Hierarchical Clustering Analysis with LC-ESI-QTOF-MS/MS. *Food Chem.* **2024**, *441*, 138320.

(26) Vaz, A. A.; Bellí, G.; Oms-Oliu, G.; Martín-Belloso, O.; Odriozola-Serrano, I. Exploring the Prebiotic Potential of Unpurified Apple Dietary Fibre Concentrate. *LWT* **2025**, *222*, 117608.

(27) Holland, C.; Ryden, P.; Edwards, C. H.; Grundy, M. M. L. Plant Cell Walls: Impact on Nutrient Bioaccessibility and Digestibility. *Foods* **2020**, *9* (2), 201.

(28) Patova, O. A.; Feltsinger, L. S.; Kosolapova, N. V.; Khlopin, V. A.; Golovchenko, V. V. Properties of Cell Wall Polysaccharides of Raw Nectarine Fruits after Treatment under Conditions That Modulate Gastric Digestion. *Int. J. Biol. Macromol.* **2023**, *245*, 125460.

(29) Alongi, M.; Manzocco, L.; Comuzzi, C.; Gorassini, A.; Verardo, G.; Rossi, A.; Anese, M.; Nicoli, M. C. The Impact of Apple Destructuring and Thermal Treatment on Bioactive Compounds: The Fate of Dietary Fibre and Polyphenols in Puree and Homogenate. *Int. J. Food Sci. Technol.* **2023**, *58* (6), 3189−3200.

(30) Colin-Henrion, M.; Mehinagic, E.; Renard, C. M. G. C.; Richomme, P.; Jourjon, F. From Apple to Applesauce: Processing Effects on Dietary Fibres and Cell Wall Polysaccharides. *Food Chem.* **2009**, *117* (2), 254−260.

(31) Yu, W.; Cui, J.; Zhao, S.; Feng, L.; Wang, Y.; Liu, J.; Zheng, J. Effects of High-Pressure Homogenization on Pectin Structure and Cloud Stability of Not-From-Concentrate Orange Juice. *Front. Nutr.* **2021**, *8*, 647748.

(32) Marszałek, K.; Trych, U.; Bojarczuk, A.; Szczepańska, J.; Chen, Z.; Liu, X.; Bi, J. Application of High-Pressure Homogenization for Apple Juice: An Assessment of Quality Attributes and Polyphenol Bioaccessibility. *Antioxidants* **2023**, *12* (2), 451.

(33) Beveridge, T.; Weintraub, S. E. Effect of Blanching Pretreatment on Color and Texture of Apple Slices at Various Water Activities. *Food Res. Int.* **1995**, *28* (1), 83−86.

https://doi.org/10.1021/acsfoodscitech.6c00023
ACS Food Sci. Technol. XXXX, XXX, XXX−XXX

(34) Houben, K.; Jamsazzadeh Kermani, Z.; Van Buggenhout, S.; Jolie, R. P.; Van Loey, A. M.; Hendrickx, M. E. Thermal and High-Pressure Stability of Pectinmethylesterase, Polygalacturonase, β-Galactosidase and α-Arabinofuranosidase in a Tomato Matrix: Towards the Creation of Specific Endogenous Enzyme Populations Through Processing. *Food Bioprocess Technol.* **2013**, *6* (12), 3368−3380.
(35) Leverrier, C.; Almeida, G.; Espinosa-Mu noz, L.; Cuvelier, G. Influence of Particle Size and Concentration on Rheological Behaviour of Reconstituted Apple Purees. *Food Biophys.* **2016**, *11* (3), 235−247.
(36) Yi, J.; Kebede, B.; Kristiani, K.; Grauwet, T.; Van Loey, A.; Hendrickx, M. Minimizing Quality Changes of Cloudy Apple Juice: The Use of Kiwifruit Puree and High Pressure Homogenization. *Food Chem.* **2018**, *249*, 202−212.
(37) Westerlund, E.; Aman, P.; Andersson, R.; Andersson, R.; Rahman, S. Chemical Characterization of Water-Soluble Pectin in Papaya Fruit. *Carbohydr. Polym.* **1991**, *15*, 67−78.
(38) Gao, J.; Lin, S.; Jin, X.; Wang, Y.; Ying, J.; Dong, Z.; Zhou, W. In Vitro Digestion of Bread: How Is It Influenced by the Bolus Characteristics? *J. Texture Stud.* **2019**, *50* (3), 257−268.
(39) Ferruzzi, M. G. The Influence of Beverage Composition on Delivery of Phenolic Compounds from Coffee and Tea. *Physiol. Behav.* **2010**, *100* (1), 33−41.
(40) Baker, R. A. Reassessment of Some Fruit and Vegetable Pectin Levels. *J. Food Sci.* **1997**, *62* (2), 225−229.
(41) Garna, H.; Mabon, N.; Wathelet, B.; Paquot, M. New Method for a Two-Step Hydrolysis and Chromatographic Analysis of Pectin Neutral Sugar Chains. *J. Agric. Food Chem.* **2004**, *52* (15), 4652−4659.
(42) Englyst, H. N.; Cummings, J. H. Simplified Method for the Measurement of Total Non-Starch Polysaccharides by Gas-Liquid Chromatography of Constituent Sugars as Alditol Acetates. *Analyst* **1984**, *109*, 937−942.
(43) De Ruiter, G. A.; Schols, H. A.; Voragen, A. G. J.; Rombouts, F. M. Carbohydrate Analysis of Water-Soluble Uranic Acid-Containing Polysaccharides with High-Performance Anion-Exchange Chromatography Using Methanolysis Combined with TFA Hydrolysis Is Superior to Four Other Methods. *Anal. Biochem.* **1992**, *207*, 176−185.
(44) Garna, H.; Mabon, N.; Nott, K.; Wathelet, B.; Paquot, M. Kinetic of the Hydrolysis of Pectin Galacturonic Acid Chains and Quantification by Ionic Chromatography. *Food Chem.* **2006**, *96* (3), 477−484.
(45) Scott, R. W. Colorimetric Determination of Hexuronic Acids in Plant Materials. *Anal. Chem.* **1979**, *51* (7), 936−941.
(46) Rosenbohm, C.; Lundt, I.; Christensen, T. M. I. E.; Young, N. W. G. Chemically Methylated and Reduced Pectins: Preparation, Characterisation by 1H NMR Spectroscopy, Enzymatic Degradation, and Gelling Properties. *Carbohydr. Res.* **2003**, *338* (7), 637−649.
(47) Niu, H.; Dou, Z.; Hou, K.; Wang, W.; Chen, X.; Chen, X.; Chen, H.; Fu, X. A Critical Review of RG-I Pectin: Sources, Extraction Methods, Structure, and Applications. *Crit. Rev. Food Sci. Nutr.* **2024**, *64* (24), 8911−8931.
(48) Chen, M.; Falourd, X.; Lahaye, M. Sequential Natural Deep Eutectic Solvent Pretreatments of Apple Pomace: A Novel Way to Promote Water Extraction of Pectin and to Tailor Its Main Structural Domains. *Carbohydr. Polym.* **2021**, *266*, 118113.
(49) Buergy, A.; Rolland-Sabaté, A.; Leca, A.; Falourd, X.; Foucat, L.; Renard, C. M. G. C. Pectin Degradation Accounts for Apple Tissue Fragmentation during Thermomechanical-Mediated Puree Production. *Food Hydrocoll.* **2021**, *120*, 106885.
(50) Zhao, J.; Zhang, F.; Liu, X.; St. Ange, K.; Zhang, A.; Li, Q.; Linhardt, R. J. Isolation of a Lectin Binding Rhamnogalacturonan-I Containing Pectic Polysaccharide from Pumpkin. *Carbohydr. Polym.* **2017**, *163*, 330−336.
(51) Zhang, H.; Chen, J.; Li, J.; Yan, L.; Li, S.; Ye, X.; Liu, D.; Ding, T.; Linhardt, R. J.; Orfila, C.; Chen, S. Extraction and Characterization of RG-I Enriched Pectic Polysaccharides from Mandarin Citrus Peel. *Food Hydrocoll.* **2018**, *79*, 579−586.
(52) Cho, E. H.; Jung, H. T.; Lee, B. H.; Kim, H. S.; Rhee, J. K.; Yoo, S. H. Green Process Development for Apple-Peel Pectin Production by Organic Acid Extraction. *Carbohydr. Polym.* **2019**, *204*, 97−103.
(53) Mao, Y.; Millett, R.; Lee, C. S.; Yakubov, G.; Harding, S. E.; Binner, E. Investigating the Influence of Pectin Content and Structure on Its Functionality in Bio-Flocculant Extracted from Okra. *Carbohydr. Polym.* **2020**, *241*, 116414.
(54) Gawkowska, D.; Cybulska, J.; Zdunek, A. Structure-Related Gelling of Pectins and Linking with Other Natural Compounds: A Review. *Polymers* **2018**, *10* (7), 762.
(55) Larsen, F. H.; Blennow, A.; Engelsen, S. B. Starch Granule Hydration-A MAS NMR Investigation. *Food Biophys.* **2008**, *3* (1), 25−32.
(56) Bushneva, O. A.; Ovodova, R. G.; Shashkov, A. S.; Ovodov, Y. S. Structural Studies on Hairy Region of Pectic Polysaccharide from Campion Silene Vulgaris (Oberna Behen). *Carbohydr. Polym.* **2002**, *49*, 471−478.
(57) Gloaguen, V.; Brudieux, V.; Closs, B.; Barbat, A.; Krausz, P.; Sainte-Catherine, O.; Kraemer, M.; Maes, E.; Guerardel, Y. Structural Characterization and Cytotoxic Properties of an Apiose-Rich Pectic Polysaccharide Obtained from the Cell Wall of the Marine Phanerogam Zostera Marina. *J. Nat. Prod.* **2010**, *73* (6), 1087−1092.
(58) Ishii, T.; Yanagisawa, M. Synthesis, Separation and NMR Spectral Analysis of Methyl Apiofuranosides. *Carbohydr. Res.* **1998**, *313*, 189−192.
(59) Vidal, S.; Doco, T.; Williams, P.; Pellerin, P.; York, W. S.; O'neill, M. A.; Glushka, J.; Darvill, A. G.; Albersheim, P. Structural Characterization of the Pectic Polysaccharide Rhamnogalacturonan II: Evidence for the Backbone Location of the Aceric Acid-Containing Oligoglycosyl Side Chain. *Carbohydr. Res.* **2000**, *326*, 277−294.
(60) Speciale, I.; Notaro, A.; Garcia-Vello, P.; Di Lorenzo, F.; Armiento, S.; Molinaro, A.; Marchetti, R.; Silipo, A.; De Castro, C. Liquid-State NMR Spectroscopy for Complex Carbohydrate Structural Analysis: A Hitchhiker's Guide. *Carbohydr. Polym.* **2022**, *277*, 118885.
(61) Wefers, D.; Bunzel, M. NMR Spectroscopic Profiling of Arabinan and Galactan Structural Elements. *J. Agric. Food Chem.* **2016**, *64* (50), 9559−9568.
(62) Wefers, D.; Flörchinger, R.; Bunzel, M. Detailed Structural Characterization of Arabinans and Galactans of 14 Apple Cultivars before and after Cold Storage. *Front. Plant Sci.* **2018**, *9*, 1451.
(63) Winning, H.; Viereck, N.; Nørgaard, L.; Larsen, J.; Engelsen, S. B. Quantification of the Degree of Blockiness in Pectins Using 1H NMR Spectroscopy and Chemometrics. *Food Hydrocoll.* **2007**, *21* (2), 256−266.
(64) Sun, H. H.; Wooten, J. B.; Ryan, W. S.; Bokelman, G. H.; Åman, P. Structural Characterization of a Tobacco Rhamnogalacturonan. *Carbohydr. Polym.* **1987**, *7*, 143−158.
(65) Rodríguez-Carvajal, M. A.; Hervé Du Penhoat, C.; Mazeau, K.; Doco, T.; Pérez, S. The Three-Dimensional Structure of the Mega-Oligosaccharide Rhamnogalacturonan II Monomer: A Combined Molecular Modeling and NMR Investigation. *Carbohydr. Res.* **2003**, *338* (7), 651−671.
(66) Du Penhoat', C. H.; Michon, V.; Goldberg, R. Development of Arabinans and Galactans during the Maturation of Hypocotyl Cells of Mung Bean (Vigna Rudiafu Wilczek). *Carbohydr. Res.* **1987**, *165*, 31−42.
(67) Broxterman, S. E.; Picouet, P.; Schols, H. A. Acetylated Pectins in Raw and Heat Processed Carrots. *Carbohydr. Polym.* **2017**, *177*, 58−66.
(68) Hua, X.; Xu, S.; Wang, M.; Chen, Y.; Yang, H.; Yang, R. Effects of High-Speed Homogenization and High-Pressure Homogenization on Structure of Tomato Residue Fibers. *Food Chem.* **2017**, *232*, 443−449.
(69) Fayaz, G.; Plazzotta, S.; Calligaris, S.; Manzocco, L.; Nicoli, M. C. Impact of High Pressure Homogenization on Physical Properties, Extraction Yield and Biopolymer Structure of Soybean Okara. *LWT* **2019**, *113*, 108324.

https://doi.org/10.1021/acsfoodscitech.6c00023
ACS Food Sci. Technol. XXXX, XXX, XXX−XXX

(70) Renoldi, N.; Melchior, S.; Calligaris, S.; Peressini, D. Application of High-Pressure Homogenization to Steer the Technological Functionalities of Chia Fibre-Protein Concentrate. *Food Hydrocoll.* **2023**, *139*, 108505.
(71) Westphal, Y.; Kühnel, S.; de Waard, P.; Hinz, S. W. A.; Schols, H. A.; Voragen, A. G. J.; Gruppen, H. Branched Arabino-Oligosaccharides Isolated from Sugar Beet Arabinan. *Carbohydr. Res.* **2010**, *345* (9), 1180−1189.
(72) Zhang, P.; Zhang, Q.; Whistler, R. L. L-Arabinose Release from Arabinoxylan and Arabinogalactan under Potential Gastric Acidities. *Cereal Chem.* **2003**, *80* (3), 252−254.
(73) Nara, K.; Kato, Y.; Motomura, Y. Involvement of Terminal-Arabinose and-Galactose Pectic Compounds in Mealiness of Apple Fruit during Storage. *Postharvest Biol. Technol.* **2001**, *22*, 141−150.
(74) Wei, J.; Ma, F.; Shi, S.; Qi, X.; Zhu, X.; Yuan, J. Changes and Postharvest Regulation of Activity and Gene Expression of Enzymes Related to Cell Wall Degradation in Ripening Apple Fruit. *Postharvest Biol. Technol.* **2010**, *56* (2), 147−154.
(75) Akinrefon, O. A. Studies on the A-l-Arabinofuranosidase of Phytophthora Paimivora (Butl.) Butl. *New Phytol.* **1968**, *67* (3), 543−556.
(76) Li, C.; Cao, H.; Wu, W.; Meng, G.; Zhao, C.; Cao, Y.; Yuan, J. Expression and Characterization of α-L-Arabinofuranosidase Derived from Aspergillus Awamori and Its Enzymatic Degradation of Corn Byproducts with Xylanase. *Bioresour. Technol.* **2023**, *384*, 129278.
(77) Nogawa, M.; Yatsui, K.; Tomioka, A.; Okada, H.; Morikawa, Y. An α-l-Arabinofuranosidase from Trichoderma Reesei Containing a Noncatalytic Xylan-Binding Domain. *Appl. Environ. Microbiol.* **1999**, *65* (9), 3964−3968.
(78) Rabiti, D.; Orfila, C.; Holmes, M.; Bordoni, A.; Sarkar, A. In Vitro Oral Processing of Raw Tomato: Novel Insights into the Role of Endogenous Fruit Enzymes. *J. Texture Stud.* **2018**, *49* (4), 351−358.
(79) Kaur, L.; Boland, M. Influence of Kiwifruit on Protein Digestion. *Adv. Food Nutr. Res.* **2013**, *68*, 149−167.
(80) Bradauskiene, V.; Vaiciulyte-Funk, L.; Cernauskas, D.; Dzingeleviciene, R.; Lima, J. P. M.; Bradauskaite, A.; Tita, M. A. The Efficacy of Plant Enzymes Bromelain and Papain as a Tool for Reducing Gluten Immunogenicity from Wheat Bran. *Processes* **2022**, *10* (10), 1948.
(81) Alongi, M.; Lanza, U.; Gorassini, A.; Verardo, G.; Comuzzi, C.; Anese, M.; Manzocco, L.; Nicoli, M. C. The Role of Processing on Phenolic Bioaccessibility and Antioxidant Capacity of Apple Derivatives. *Food Chem.* **2025**, *463*, 141402.

https://doi.org/10.1021/acsfoodscitech.6c00023
ACS Food Sci. Technol. XXXX, XXX, XXX−XXX